DOE/NASA/50194-37
NASA TM-83329

Characterization of a High-Pressure Diesel Fuel Injection System as a Control Technology Option to Improve Engine Performance and Reduce Exhaust Emissions

John J. McFadden, Robert A. Dezelick,
and Richards F. Barrows
National Aeronautics and Space Administration
Lewis Research Center

March 1983

Prepared for
U.S. DEPARTMENT OF ENERGY
Conservation and Renewable Energy
Office of Vehicle and Engine R&D

NOTICE

NASA TM-83329

DOE/NASA/50194-37

L

Dupe

DISPLAY 15/2/1

83N24431** ISSUE 13 PAGE 2154 CATEGORY 85 RPT#: NASA-TM-83329 NAS 1.15:83329 DOE/NASA/50194-37 CNT#: DE-AI01-80CS-50194 83/03/00 37 PAGES UNCLASSIFIED DOCUMENT

UTTL: Characterization of a high-pressure diesel fuel injection system as a control technology option to improve engine performance and reduce exhaust emissions TLSP: Final Report

AUTH: A/MCFADDEN, J. J.; B/DEZELICK, R. A.; C/BARROWS, R. R.

CORP: National Aeronautics and Space Administration. Lewis Research Center, Cleveland, Ohio. AVAIL.NTIS SAP: HC A03/MF A01

DOE/NASA/50194-37
NASA TM-83329

Characterization of a High-Pressure Diesel Fuel Injection System as a Control Technology Option to Improve Engine Performance and Reduce Exhuast Emissions

John J. McFadden, Robert A. Dezelick,
and Richards F. Barrows
National Aeronautics and Space Administration
Lewis Research Center
Cleveland, Ohio 44135

March 1983

Prepared for
U.S. DEPARTMENT OF ENERGY
Conservation and Renewable Energy
Office of Vehicle and Engine R&D
Washington, D.C. 20545
Under Interagency Agreement DE-AI01-80CS50194

CHARACTERIZATION OF A HIGH PRESSURE DIESEL FUEL INJECTION SYSTEM AS A CONTROL TECHNOLOGY OPTION TO IMPROVE ENGINE PERFORMANCE AND REDUCE EXHAUST GAS EMISSIONS

J. J. McFadden, R. A. Dezelick, and R. F. Barrows
National Aeronautics and Space Administration
Lewis Research Center
Cleveland, Ohio 44135

SUMMARY

The Department of Energy, Division of Transportation Energy Conservation, has established several broad programs aimed at reducing highway fuel consumption. One such program is the Heat Engine Highway Vehicle Systems Program. Within that program is a subproject which addresses control technology for the reduction of particulate and gaseous emissions from Diesel engines. Program management for this project has been delegated to the National Aeronautics and Space Administration (NASA) which has a fully instrumented Diesel engine test facility at the Lewis Research Center (LeRC).

A high pressure, electronically controlled fuel injection system prototype was obtained to assess the effectiveness of high pressure, controlled rates of injection as a control technology option. Test data were obtained on a four-valve, single-cylinder, open-chamber, 1.356 liter, four-stroke cycle Diesel test engine using an inlet boost pressure ratio of 2.6:1. Engine performance and emissions data were compared against results obtained with a modified commercial, mechancial fuel injection system, optimized for performance and fuel consumption.

The mechanical fuel injection system used had two cam actuated plunger elements, operating together, and coupled to a single high pressure line, to feed a single injector for high-pressure, high-output capability. The electro-hydraulic system had supply pressures in the range of 23 to 33 MPa. These were amplified by a fluid intensifer (hydraulic amplifier) with a 4:1 area ratio that resulted in peak injection pressures of 47 to 69 MPa. The electro-hydraulic fuel injection system produces an injection pressure trace that has an increasing rate of injection followed by a sharp, fast, cut-off of injection. This is in contrast to the standard (baseline) mechanical fuel injection system used in this program that has a high initial rate of injection followed by a decreasing rate of injection.

Particulate and gaseous emissions were measured according to the EPA Federal Test Procedure (FTP), Heavy Duty Engines, for single modes of operation. The majority of data were obtained at 2500 ERPM at two loads, 690 and 955 kPa BMEP. Abbreviated timing traverses were conducted at these loads using an injection nozzle with reduced flow area. One complete test matrix was also accomplished at three speeds and three loads.

Test results at 691 kPa BMEP, 2500 ERPM, with the electro-hydraulic fuel injection system indicate that total particulates can be reduced by as much as 26 percent. The soluble organic mass fraction of the particulates are reduced by as much as 42 percent; however, the solid mass fraction of the total particulates increased 34 percent. For the gaseous emissions, oxides of nitrogen are reduced by 35 percent, hydrocarbons by 53 percent, and carbon monoxide by

E-1576

53 percent below baseline emissions developed with the mechanical system. At 930 kPa BMEP and 2500 ERPM, reductions in total particulates with the electro-hydraulic injector are insignificant (3 percent). The soluble organic mass fraction of the total particulates is reduced 38 percent; however, the solid mass fraction of the total particulates increased by 19 percent above the baseline solid mass fraction. Oxides of nitrogen are reduced by 40 percent, hydrocarbons by 64 percent, and carbon monoxide by 57 percent below baseline.

The ramped, increasing rate of initial injection characteristic of the electro-hydraulic fuel injection system, when controlled in such a way that the point of peak injection pressure occurs in the vicinity of top dead center, can significantly reduce both particulate and oxides of nitrogen emissions. The sharp cut-off pressure collapse characteristic is conducive to significant reductions in hydrocarbon, carbon monoxide and the soluble organic mass fraction of the particulates. These injection characteristics also show reduced cylinder pressures of 11 percent and 14 percent at 691 kPa and 930 kPa BMEP respectively. No significant improvements were found however, in either engine performance or fuel consumption.

It was determined during the test program that increasing supply pressure to the electro-hydraulic injector does not necessarily increase the peak injection pressure. It can, however, increase the rate of injection which effectively advances the timing of the injection event. This promotes early ignition that results in increased oxides of nitrogen formation. The effect of retarded injection timing under this condition was not completely explored. However, reducing the injection nozzle tip flow area by 23 percent decreased the rate of injection and thereby increased the peak injection pressure. Oxides of nitrogen formation was found to be a function of the rate of injection and the point in the cycle where peak injection pressure occurs.

INTRODUCTION

The Department of Energy, Division of Transportation Energy Conservation, has established several broad programs aimed at reducing highway fuel consumption. One such program is the Heat Engine Highway Vehicle Systems Program. Within that program is a subproject which addresses control technology for the reduction of particulate and other emissions from Diesel engines.

One of the National Aeronautics and Space Administration (NASA) programs underway at the Lewis Research Center (LeRC) is directed at developing the technologies for reducing fuel consumption and exhaust emissions for lightweight diesel aircraft engines for general aviation use. One accomplishment of this program to date has been the construction and development of a fully instrumented, single cylinder, diesel engine test facility. Because of the similarity in objectives between advanced automotive type and aircraft diesel engine technology, it was determined technically feasible and cost effective to combine selected NASA research efforts with those of the Department of Energy (DOE). This particular program was sponsored by DOE.

High pressure and controlled rates of fuel injection enhances the true potential of distillate fueled compression ignition engines (ref. 1). Theoretically, high pressure fuel injection may also extend the rated speed capability of open chamber combustion systems, decrease the power to weight ratio, provide improved fuel-to-air mixing, and potentially improve combustion efficiency and emissions. Only a limited number of electronically controlled high pressure

systems are available for research studies, and only a minimal amount of literature has been published to report actual experience or engine testing with the electro-hydraulic/fuel intensifier concept. References 2 and 3 are two recent examples of such studies.

The development of high speed, high power-to-weight, fuel efficient diesel engines for aircraft and automotive type use requires a fuel injection system that can provide higher rates of injection compatible with the physical and temporal constraints of intermittent combustion, open chamber diesel engines. Fuel injection systems, commercially available, are generally limited either because of weight and cost penalties, as with unit injectors; or because of pressure and speed limitations, as with in-line and rotary type pumps.

This report describes the investigation and characterization of a high pressure, electro-hydraulic, prototype fuel injector on a single cylinder diesel research engine. The injection system electronically controls the fuel metering and injection timing requirements of the engine by means of electrical solenoids. The experimental electronically controlled system used in this study provides hydraulic pressure intensification at the injector by means of a fluid transformer or differential area plunger. Injection pressure levels are then a function of the supply pressure and the area ratio of the piston intensifier and plunger. Test data reported here does not compensate for the additional power required to drive the high pressure fuel supply system, but this is not considered relevant to the data obtained.

The amount of data obtained and analyzed in this study, using the electro-hydraulic fuel injector, is limited because of the lack of system durability under boosted inlet conditions. The report presents those data points obtained with the electronically controlled injector and compares these results with baseline tests conducted with a special in-line mechanical pump, operating with two plungers in parallel. Baseline data were developed for optimun BSFC. Testing and adjustment of the electronic injection system was in accordance with the manufacturer's recommendations. No extensive effort was attempted to apply special instrumentation for diagnostic purposes, or otherwise revise the design of the electro-hydraulic system because of limiting time constraints in the program.

SYMBOLS

ERPM	engine speed rpm
P_i	engine inlet air pressure (kPa)
Pe	engine exhaust back pressure (kPa)
CYLPEAK	peak cylinder gas pressure (kPa and degrees after TDC)
INPEAK	peak injection pressure (MPa and degrees before TDC)
BSPM	brake specific total particulate matter (g/kW-hr)
BSCO	brake specific carbon monoxide (g/kW-hr)
BSHC	brake specific hydrocarbons (g/kW-hr)
BSNOX	brake specific oxides of nitrogen as NO (g/kW-hr)
SOF	soluble organic fraction of total mass particulate matter (percent or g/kW-hr)

DESCRIPTION OF RESEARCH FACILITY AND INSTRUMENTATION

The NASA Lewis Research Center diesel engine test facility consists of a single cylinder research engine, an inlet air processing system, a fuel supply system, a water cooling system, a lubricating oil system, a monitoring system for engine parameters, an exhaust emissions sampling system, and a real time data acquisition and processing system. Figure 1 shows the engine located in the test facility.

Engine Specifications

The test engine is an open chamber, single cylinder engine with a controlled inlet pressure of 262 kPa and exhaust pressure of 207 kPa ($P_i/Pe = 1.27$). The engine is coupled to an eddy current dynamometer with 22 kW motoring and 112 kW absorbing capability. Other engine specifications are:

No. Cylinders	1
Bore	120 mm
Stroke	120 mm
Displacement	1.357L
Maximum Speed	3000 rpm Full Load
Cylinder Head	Four Valve (Two Intake, Two Exhaust)
Compression Ratio	17.29:1
Combustion Chamber	Bowl in Piston

Fuel Injection System

The conventional mechanical cam actuated plunger fuel injection system supplied with the engine, and used for baseline tests, was optimized for engine performance and comprised the following:

Fuel Injection Pump and Governor Assembly	Mechanical (two elements in parallel)
Fuel Injection Nozzle:	Five hole at 0.36 mm diam, 2.8 L/D (Sac volume = 1.5 mm^3)
Nozzle Opening Pressure:	26 MPa
Timing Advance:	Manual
Fuel Injection Line:	6 mm X 2 mm X 600 mm

Inlet Air System

Simulated turbocharged engine inlet air is supplied from the building plant

air supply. The air flows through a steam humidifying chamber (to control relative humidity), through a heater, then a surge tank, and finally into the engine. No arrangement is made for cooling the air below ambient conditions.

Fuel Supply System

The fuel system is supplied from two 55 gallon drums which store DF-2 reference fuel. Fuel properties are listed in table I. The fuel flows through a positive displacement fuel metering system to a vented float chamber located on the wall about six feet above the floor, and from the float chamber the fuel passes to the test engine. Fuel rates are transmitted electronically to the data acquisition system and displayed on the cathode ray tube (CRT) at the test console in both lb/hr and in μL/injection.

Viscosity, cs	3.80
Specific gravity	0.8516
H/C mass ratio	1:6.7
Saturates, vol. percent	75.10
Olefins, vol. percent	2.48
Aromatics, vol. percent	22.42
Sulfur, wt. percent	0.29
Gross heat value, J/kg (Btu/lbm)	$44X10^6$ (19,034)

Water Cooling System

The engine and dynamometer are water cooled. The cooling water system consists of a flow meter, atmospheric head tank (located approximately 8 feet above the test cell floor), circulating pump, two heat exchangers, piping, regulators, and various instruments and controls. Although tied in with the base supply and return lines, it is a bifurcated system; one for the engine and the other for the dynamometer. A large heat exchanger is used to dissipate the power from the dynamometer while a smaller heat exchanger is used for the engine.

Lubricating Oil System

The engine lubricating system has a capacity of 14 liters and contains an engine driven oil pump, filter, oil cooler, and a heater with provisions for oil temperature control.

Engine Data Monitoring System

The engine and ancillary equipment are monitored by thermocouples, pressure pick-ups and other transducers for measuring test parameters. The data acquisition system is arranged to collect five consecutive sets of data for each test point in less than one second. The mean and standard deviation values are printed out for each of 154 different test parameters. The test parameter values are displayed on the engine control console and on a cathode ray tube (CRT). Calculated test results are also displayed on a CRT and can be reproduced at a typewriter terminal on command to provide a hard copy of the data.

A NASA designed Modular Engine Instrumentation System (MEIS) (ref. 4) is used to provide pressure-volume (PV) and log function of the pressure and volume diagrams. The diagrams are displayed on and photographed from an oscilliscope. The data is updated every cycle. The tangent of the log function of pressure and volume, available from the oscillograph display or a polaroid print, may be used to evaluate an on-line value of the cylinder gas polytropic exponent for any particular portion of the pressure-volume trace. The main modular unit displays indicated mean effective pressure (IMEP). Associated modules display peak cylinder gas pressure (CYLPEAK), peak injection pressure (INPEAK), and the number of degrees after or before top dead center where peak pressure occurs.

All instrumentation is connected to a centralized data collection system named ESCORT. A remote acquisition micro-processor (RAMP), located in the test facility, serves as an interface between the facilities instrumentation and one of a pool of minicomputors located in another building. The minicomputor performs Those calculations required for on-line test monitoring and provides engineering unit displays for viewing on CRTs in the test facility. Selected portions of the data are recorded by a signal to the minicomputor which then passes the data to a data collector system for recording on magnetic tape.

The data from the tape is then transfered to an IBM 370/67 computer for final processing. The ESCORT system, also provides digital signal conditioning and calibration. For calibration, the facility is placed in a null position and zero data are taken. The "RCAL" resistors are automatically switched in, and the span data are taken. The correction factor for each channel is then calculated, stored, and recorded on the data collector for use in the central data reduction system. These values are checked against two baseline sets of values for drift, and any channel that exceeds a 2 percent change is identified.

Exhaust Emissions Sampling System

As shown in figure 2, the exhaust leaving the engine enters a surge tank, from here it passes through an in-line opacity meter, and is finally exhausted to the atmosphere outside of the test cell. The engine exhaust system is also arranged so that a controlled volume fraction of the total engine exhaust is routed through an orifice to a second opacity meter, to the dilution tunnel, and exited through a blower to the atmosphere outside of the test cell.

Hot exhaust gas samples are fed through a heated line (190° C) to an emissions measurement console which contains the following instrumentation:

Nondispersive Infrared Analyzer for CO_2
Nondispersive Infrared Analyzer for CO
Heated Chemiluminescence for NO/NO_x
Paramagnetic Oxygen Analyzer for O_2
Heated Flame Ionization Analyzer for HC

The exhaust emissions system is designed to provide exhaust gas analysis data and proportional mass particulate collection. A view of the test operators console, instrument panel and emissions console are shown in figure 3. The particulates are sampled from a 25.4 cm diam X 305 cm stainless steel exhaust sampling section shown in figure 4. Other specifications of the tunnel are as follows:

Maximum tunnel flow.....0.5 m^3/s
Pump displacement per revolution....0.017 m^3
Pump heater rating.....12K w max
Max probe temp.....51.7° C
Inlet filter area.....434 cm^2
Extraction probe.....1.59 cm diam

Particulate Measurement

Particulate emissions from diesel engines are complex mixtures of solid and liquid compounds. The solid fraction of particulate emissions are primarily carbonaceous and the liquid fraction is comprised primarily of organics and sulfates. The particulate matter contributes to the total suspended ambient particulate concentration and the soluble organics have been shown to correlate with mutagenic activity (ref. 5). In this report, the solid fraction correlates with smoke opacity and the organic fraction correlates with the gaseous phase HC formation.

Particulates can be collected by means of an automatic remotely-controlled filtering cassette. In these tests, collecting of particulate samples was accomplished by using two discrete 47 mm samplers, in series, to minimize data variability and to provide a back-up filter for determining collection efficiency. This modification is shown in figure 5.

Fluorcarbon coated glass fiber filters (47 mm diam.) were used to collect the particulate matter for physical characterization. As shown in figure 2, the diluted exhaust gas sample is drawn through one of two extraction probes in the dillution tunnel to the appropriate filter. The diluted sample is continuously drawn through a by-pass filter to the exhaust system, except during the sampling mode. During sampling, the diluted sample is drawn in series through two 47 mm discrete in-line samplers (shown in fig. 5) and exhausted to the atmosphere. The diluted exhaust sample was maintained at or below 52° C. The optimun sample time was determined to be 400 seconds to collect an adequate mass sample (>1.5 mg) of particulate matter. The filters were conditioned in a humidity chamber for 24 hours prior to weighing and particulate collection. After collection, the filters were again stored in a humidity chamber to stabilize mass to the original humidity before weighing. Total particulate mass from each test was determined by adding the particulate mass from both the primary and back-up filters. A representative number of filters were placed in glass Soxhlet micro-extractors and the soluble organic fraction (SOF) was extracted

using dichloromethane solvent. The samples were then reconditioned in the humidity chamber, and reweighed. The difference in mass between the Total Particulate Matter (TPM) and the soluble organic material (SOM) represents the unextractable residue, or solid mass fraction of the TPM (ref. 6).

The microbalance used for this measurement is accurate to ±0.01 mg. The net weight of the total particulate mass, the sample probe flow volume that passed through the filter, and the sample time are recorded manually and entered into the data collector system for processing. The soluble organic and solid mass fractions of the TPM are manually recorded.

DESCRIPTION OF ELECTRO-HYDRAULIC HIGH PRESSURE FUEL INJECTION SYSTEM

The system used for testing and evaluation on the single cylinder test engine consisted of the following major items:

1. Solenoid controlled injector.
2. High pressure (35 MPa maximum) supply pump system.
3. Low pressure supply pump system for fuel metering (2.5 MPa)
4. Line accumulator for pressure dampening.
5. Electronic control unit.
6. Remote control unit for timing and fuel control.

A schematic arrangement of the electro-hydraulic system is shown in figure 6; the hydraulic circuit is shown in figure 7; and the injector is shown in figure 8 as it was installed on the single cylinder test engine.

Electronic logic programs the operation of two solenoid operated valves in the injector. The accumulator valve supplies fuel under pressure to the top of the intensifier piston (10 mm diam) during the injection process. The drain valve relieves fuel pressure from the top of the intensifier piston during the metering portion of the cycle. The plunger (5 mm diam) is moved upward by low pressure fuel (2.5 MPa) and positioned electronically for fuel metering as determined by the setting on a remote controlled electronic pot. Injection timing control is also accomplished by the dial setting of a second remote controlled electronic pot.

TEST RESULTS

The injectors and the conditions under which these were tested are summarized in table II. The results of testing two electro-hydraulic injectors with numerous adjustments are presented in table III. The injection pressure characteristics were changed for each injector repair/adjustment because of different accumulator supply pressure and disassembly/readjustment of the solenoid valves.

Each set of data developed with the electro-hydraulic system is compared to baseline test data obtained with the mechanical injection pump supplied with the single cylinder engine, which was optimized for fuel consumption and engine performance (ref. 7). The engine was supercharged to a 2.6:1 boost pressure ratio, retaining an intake to exhaust pressure ratio ($P_i/Pe = 1.27$) at each load and speed.

Electro-Hydraulic Injector A Test Results - 5 Hole Nozzle

The initial sequence of tests conducted with injector A were intended to simulate mean peak injection pressures developed with the mechanical system (~ 40 MPa at 690 kPa BMEP and 2500 ERPM). This was to establish a reference for evaluating the effect of increased injection pressure. An accumulator supply pressure of 23 MPA on top of the intensifier piston produced a peak injection pressure (INPEAK) of 47 MPa, but this resulted in unstable engine operation and variability in the data. The electro-hydraulic system, operating at 23 MPa supply pressure, was also sensitive to air ingestion into the fuel supply system resulting in frequent operational malfunctions and shutdowns. This condition was appraised to be a consequence of nozzle valve imbalance caused by pressure fluctuations above the nozzle valve, compounded by high compression/combustion pressures under the nozzle valve seat. Only two test points were obtained at 23 MPa supply pressure (table III), but these did indicate potential reductions in BSPM (total particulate, 45 percent), in the soluble organic mass fraction of the particulates (78 percent), BSNOX (39 percent), and BSCO (68 percent).

A typical pressure versus crank angle diagram for the electro-hydraulic fuel injector is shown in figure 9 compared against the mechanical system for the same fuel rate and speed; i.e., 80 μL/injection at 2500 ERPM. An explanation of the fuel injection events for both the mechanical and electro-hydraulic systems is shown. It should be noted that the scale factor for the pressure transducers for each system are different. For the mechanical system, the injection fuel pressure scale on the oscillograms factor is 13.8 MPa per division and for the electro-hydraulic system 20.7 MPa per division. Cylinder gas pressure transducers, however, do have the same scale. The oscillogram for the mechanical system includes a nozzle valve lift diagram along with the injection and cylinder pressure wave characteristics. The oscillograms for the electro-hydraulic system do not show the movement of the nozzle valve, but instead show the downward ramp movement of the intensifier plunger. The height of the ramp is proportional to plunger lift which is determined by the fuel pot setting.

Peak injection pressure with the mechanical system normally occurs at the point in the cycle when the nozzle valve reaches maximum lift position. The injection pressure profile of the electro-hydraulic injector, is considerably different. Peak pressure occurs later in the cycle and is more closely coincident with the end of injection and beginning of ignition. The beginning of injection for the electro-hydraulic system was interpreted to be 18° CA-BTC, the same as with the mechanical system.

The significant reductions shown in table III for HC, CO and soluble organics for this first sequence of tests are mostly attributed to the rapid closing action characteristic of the electro-hydraulic nozzle valve. The reduction in BSNOX is attributed to the slow initial rate of injection or slow rate of injection pressure rise. This is signified by the retarded point of peak injection pressure (9° CA later in the cycle) which reduced the peak combustion gas pressure by about 17 percent (fig. 10). Independent variables, ERPM, BMEP, and A/F ratio showed a wide range of variability and these results can be considered only directional.

The second sequence of tests with injector A was accomplished with an air-driven high pressure supply pump and with an increase in accumulator supply

pressure to 28 MPa. With the higher supply pressure, peak injection pressure increased almost proportionately from 47 MPa at a supply pressure of 23 MPa, to 58 MPa at a supply pressure of 28 MPa. With a 4:1 intensifier to plunger area ratio, the injection pressure increase for this injector is on the order of only 2:1, about 50 percent intensifier efficiency. This low efficiency is attributed to a combination of the pressure drop across the accumulator valve and internal leakage within the injector body.

At 80 μL/injection, 2500 ERPM (fig. 11), the general trend for emissions continue to be significantly lower than the mechanical baseline reference and reasonably close to those levels obtained with the injector operating at 23 MPa supply pressure. For a 23 percent increase in injection pressure, the only obvious effects were marginal increases in the mean values of BSCO, BSPM and soluble organics. For the same equivalent point of beginning of injection, the injection peak was slightly advanced, about 1° CA, but the duration of injection is interpreted to be about the same as for the injector at 23 MPa supply pressure.

Compared to the baseline mechanical system at 690 kPa BMEP, 2500 ERPM, emissions from the engine using injector A result in a 26 percent reduction in total particulates. The soluble organic mass fraction of the particulates is reduced 42 percent below the baseline soluble fraction, while the solid mass fraction increased by 34 percent. BSNOX were reduced 35 percent, BSHC 53 percent, and BSCO 53 percent. The peak cylinder gas pressure with injector A was 14 percent lower. BSFC is approximately 2 percent lower, but within the range of experimental error.

At 100 μL/injection, 2500 ERPM, with 28 MPa supply pressure, when compared to the mechanical baseline emissions, total particulates are reduced only 3 percent. The solid mass fraction portion of particulates however, is 19 percent higher than the baseline solid fraction. The soluble organic mass fraction portion however, is 38 percent lower, BSNOX 40 percent lower, BSHC 64 percent lower, and BSCO 57 percent lower than baseline emissions (fig. 11). Average BMEP of 930 kPa is 3 percent lower than the mechanical baseline system, but fuel consumption is about the same. Peak cylinder pressure is also lower by about 11 percent. It is observed in figure 12 that the injection peak occurs at a mean value of 5° CA-BTC compared to 15° CA-BTC with the mechanical system, and the total duration of injection is interpreted as being about 4° CA shorter.

The primary difference in the operational characteristics of the mechanical system and the electro-hydraulic system, other than injection pressure, is the injection pressure profile. For the mechanical system at 80 or 100 μL/injection (2500 ERPM), the injection pressure decreases, and for the electro-hydraulic system counterpart, pressure increases during the injection process. The inference here is that with the conventional cam actuated plunger, the initial rate of injection is very high and earlier in the compression cycle which causes high rates of heat release before top dead center. With the ramped increasing rate of injection characteristic of the electro-hydraulic system, the maximum rate of injection occurs later, close to top dead center. This provides a more controlled rate of heat release as found with pilot injection, fumigation or with other charged air preparation techniques. It can also be observed from the pressure diagrams that ignition occurs at or close to the point of peak injection pressure with the electro-hydraulic injector, or that point in the cycle when the rate of injection is the highest. Consequently, the initial rate of cylinder gas pressure rise (heat release) is less, peak combustion pressure is reduced by 11 to 13 percent, and BSNOX is reduced 35 to 40 percent. The sharp pressure cut off at the end of injection, which is characteristic of the electro-hydraulic system, obviously is conductive to the lower hydrocarbon, SOF, and carbon monoxide emissions.

The third sequence of tests with injector A was with the accumulator supply pump pressure increased from 28 to 33 MPa. The same timing (equivalent to 18° CA-BTC beginning of injection) was retained. Even though the accumulator supply pressure increased 18 percent, it actually produced 4 to 8 percent lower peak injection pressures. One obvious difference in the injection pressure trace with 33 MPa supply pressure (fig. 13) is the higher initial rate of pressure rise and less obvious point of pressure transition at 18° CA-BTC, or that point in the cycle interpreted as beginning of injection. With the mechanical system, the valve lift diagram provides a convenient and accurate way to determine the injection value timing response. With the electro-hydraulic system, interpretation of the hydraulic pressure diagram may not be as accurate. With the other tests, the beginning of injection was interpreted as occurring after the first pressure plateau as shown in figure 9. With the higher supply pressure (33 MPa), this is not as well defined. However, the timing pot setting was the same, and the beginning of injection pressure rise (22° CA-BTC) remained the same. The lower peak injection pressure is probably a result of the higher rate of injection. This advances the point at which the peak injection pressure occurs (9° CA versus 5° CA-BTC with 28 MPa supply pressure at 100μL/injection) and provides a shorter duration of injection. The point of ignition is again observed to occur close to the point of peak injection pressure. It can also be observed in figure 13 that there is some evidence of plunger bounce near the end of injection. This may or may not affect the injection process (or otherwise induce post injection). Since the hydrocarbon levels were not significantly affected, and remain well below the baseline hydrocarbon level, this anomaly is interpreted to be contained within the injector and not enough to unseat the nozzle valve.

As shown in figure 11, BSPM, the soluble organic fraction, BSHC and BSCO remain significantly lower than the baseline emissions. BSPM is 44 percent lower, the soluble organic mass fraction is 65 percent lower, BSHC is 52 percent lower, and BSCO is 50 percent lower than the baseline at 714 kPa BMEP, 2500 ERPM. At the higher load, 954 kPa BMEP, BSPM is 18 percent lower, the soluble organic mass fraction 70 percent lower, BSHC 41 percent lower, and BSCO 42 percent lower than the comparable baseline values. BSNOX, however, increased from an average of 11 gm/kW-hr at the lower supply pressure to 17.5 gm/kW-hr at this higher supply pressure. This represents an increase in BSNOX of 59 percent as a result of increasing the accumulator supply pressure and readjusting both the drain valve and the accumulator valve solenoids. An increase in the rate of injection effectively shortened the duration of injection and advanced the point where end of injection occurred. This contributed to the increase in rate of pressure rise in the cylinder and to a significant increase in the formation of oxides of nitrogen, even though the interpreted point for beginning of injection did not change. BMEP and BSFC are directionally favorable but within the range of experimental error.

Operation of injector A with 33 MPa supply pressure was accomplished at three different speeds and loads. The results (mean values) of these tests are shown in figures 14 to 16 and are compared against data developed with the baseline system, optimized for BSFC and performance. The data are also shown in table IV. Engine operation at the higher loads with this configuration was especially unstable, and it was difficult to stabilize load and speed points. This may be a consequence of attempting to operate the system at maximum fuel delivery and without excess accumulator supply pump capacity. BSPM values are not much different from the baseline counterpart, nor was the soluble organic fraction significantly different, except at 2500 ERPM where the SOF is apparently more responsive to the decreased HC. BSHC levels continued to be 35 per-

cent to 67 percent lower than the baseline results at all loads and speeds. BSCO emissions are 17 percent to 48 percent lower than baseline values at 1500 and 2500 ERPM but are essentially the same as baseline data at 2000 ERPM for the higher loads. BSNOX values are significantly higher at 1500 ERPM, and higher than or equal to the baseline values at 2000 and 2500 ERPM. Engine performance trends are essentially the same except for 1500 and 2000 ERPM, where the electro-hydraulic system was very unstable at the higher loads and resulted in reduced power or BMEP. These tests were conducted with the highest recommended accumulator supply pump pressure and, as expected, produced higher rates of injection. Peak injection line pressures were not too different from the baseline system except at the lighter loads and at the lower speed (1500 ERPM). In general, higher supply pressure continued to provide reductions in BSCO and BSHC. BSNOX emissions, however, increased with the higher rate of injection. Although the point of the initial rate of pressure rise (equivalent to conventional port closing) was the same, heat release in the cylinder was more rapid and the peak cylinder pressure increased by about 20 percent. It can also be observed that the normal trade-off between NO_x and BSFC does not appear to prevail for the conditions tested with this electro-hydraulic injector.

Electro-Hydraulic Injector B Test Results - 8 Hole Nozzle

The fourth sequence of tests using injector B was conducted with a different injector nozzle drilling configuration (8 holes at 0.25 mm diam). This nozzle, with a 23 percent decreased flow area, was configured in an effort to further explore the effects of higher injection pressure. Test results were compared to baseline data conducted with the 5 hole nozzle. The test results at 2500 ERPM are shown in table III. Two tests were initially conducted at 80 μL/injection. Readjustment of both solenoid valves on the injector was required to stabilize the engine at higher loads, i.e., 100μL at 2500 ERPM. Of the two initial tests with injector B, one was conducted with a supply pressure of 28 MPa, the other with 33 MPa supply pressure. The pressure versus crank angle diagrams for these two tests are compared in figure 17. The increase in injection peak pressure (INPEAK) is proportional to the increase in supply pressure, but the duration of injection appears to be about the same. BSPM, BSHC, and BSCO are greatly reduced on the average by 55 percent, 83 percent, and 77 percent, respectively. BSNOX at either pressure is higher than the baseline system by 14 to 25 percent. Some improvement in BMEP and BSFC (3 percent) is indicated for the higher pressure.

The fifth sequence of tests was conducted after readjusting both injector solenoids, and two tests were conducted with 28 MPa supply pressure at the higher load (100 μL/injection). Improvements were noted in both engine performance and emissions (table III). As in the previous tests, BSPM, BSHC and BSCO are reduced 67 percent, 75 percent and 78 percent respectively; but following this adjustment of both the injector solenoids, BSNOX was also reduced 34 percent below baseline. The reduction in BSNOX is interpreted to be a result of the slower rate of injection which is a function of supply pressure above the intensifier piston, flow rate through the solenoid valve, and the nozzle flow area. The most outstanding differences in injection characteristics appear to be the smoother, slower rate of injection pressure rise; the retarded point of peak injection pressure; and lower nozzle opening pressure (figure 18). Peak cylinder pressure was 10 percent lower than baseline. It is not possible

to assess what, if any, advantage could be attributed to the 8 hole nozzle configuration. Some plunger bounce is in evidence, but the low HC indicates that the nozzle valve probably remained closed at the end of injection and was not adversely affected by the magnitude of the late pressure wave.

The sixth and final sequence of tests was conducted with injector B after the drain valve solenoid was readjusted. Until this time in the program, all tests at 2500 ERPM were conducted at the same injection timing. This last sequence of tests was conducted at two loads with the electronic timing adjusted for 16° CA, 18° CA and 20° CA-BTC beginning of actual injection of fuel. At the equivalent 18° CA-BTC timing used for the previous test, injection peak pressure occurred about 1° CA earlier in the cycle, the injection pressure trace is essentially the same, and the duration of injection appears to be a few degrees shorter (figure 19). As shown in table III, however, particulates, CO and HC increased significantly. BMEP is about 3-1/2 percent lower, and BSFC is about 6 percent higher. BSNOX also increased 11 percent from 11.4 to 12.7 gm/kW-hr. This deterioration in both performance and emissions is not explainable from the pressure diagrams. The increase in BSNOX may be consequence of the higher (~5 percent) rate of injection. The increased BSPM, BSHC and BSCO could be a consequence of plunger bounce from the reflected pressure wave at the end of injection, resulting in either a secondary injection or extended duration of the main injection. As compared to the baseline 5 hole nozzle data, for 100μL/ injection, BSNOX is 27 percent lower, but engine performance and other emissions are about the same for 18° CA-BTC timing. As injection timing was retarded only 2° CA, a further reduction in BSNOX was evidenced (fig. 20). Advancing the injection timing 2° CA showed marginal improvement in engine performance at 100 μL with a 23 percent penalty in BSNOX emissions. Other emissions remained essentially unchanged. At 80 μL/injection (2500 ERPM), BSPM increased by 47 percent, but BSNOX, BSHC, and BSCO emissions are 18 percent, 30 percent, and 48 percent, respectively, lower than baseline for equivalent 18° CA-BTC timing. By retarding the injection timing only 2° CA, BSNOX is further reduced as expected, but without any penalty in engine performance. Advancing the injection timing 2° CA increased BSNOX but again did not significantly affect engine performance.

Discussion

The electro-hydraulic injector/pressure intensifier concept produces an injection pressure trace with an increasing rate of injection such that the maximum rate of injection occurs later in the cycle and closer to top dead center when compared to the conventional system. Consequently, it can be shown that the magnitude of BSNOX emission correlates with that point in the cycle where peak injection pressure (INPEAK) occurs. This correlation is shown in figure 21 for the two different injector configurations at 2500 ERPM. Peak injection pressure timing affects the formation of oxides of nitrogen and is a variable sensitive to adjustment of the solenoid valves, flow rate to the top of the intensifier piston, and rate of injection. Engine performance parameters, BMEP and BSFC, do not appear to be especially sensitive to peak injection pressure timing for this series of tests. As demonstrated, increased supply pressure to the intensifier does not necessarily increase injection pressure, but can increase the rate of injection and adversely affect NOX formation at equivalent injection timing settings. The outstanding feature of the electro-hydraulic

intensifier is the ability to provide a very sharp and abrupt end of injection which promotes significant reductions in CO, HC and SOF. This feature, however, is found to be a function of the specific injector variation and susceptible to pressure wave reflections that can react on the plunger to allow post injection, or otherwise extend the duration of injection. This irregularity can result in increased HC, CO, and particulate emissions. The SOF, a function of HC, can also be adversely affected.

As with any high pressure diesel fuel injection system, the rate and duration of injection are a function of pressure and nozzle flow area. With the electro-hydraulic injector tested in this program, the rate and duration of injection is a function of supply pressure, flow rate to the intensifier piston, and nozzle flow area. For best overall engine and emissions performance, any variation in these independent variables require controlled regulation of the injection timing event. Additional work is needed to fully explore the total effect of each of these variables for optimum results under different operating conditions. The slow beginning, fast end of injection characteristic, however, does provide the potential for significant reductions in exhaust emissions from diesel engines. Of particular interest are NOX, and total particulates which are difficult to control in a diesel engine without trade-off penalties. In one example, these were each reduced significantly below baseline emissions with no obvious penalty in engine performance and with significant reductions in other emissions; i.e., CO, HC and SOF.

CONCLUSIONS

Engine performance and exhaust emissions data developed with the electro-hydraulic injector/pressure intensifier were compared to that obtained with the conventional mechanical injector (optimized for BSFC). The electro-hydraulically controlled injector develops a triangular injection pressure characteristic with a slow rate of pressure rise ($\Delta P/\Delta t$) followed by a steep rate of pressure collapse, or slow beginning-fast end of injection. This is in contrast to the fast beginning-slow end of injection characteristic of the conventional mechanical fuel injection system.

Analysis of the data led to the following conclusions:

1. Test results with the electro-hydraulic/pressure intensifier, high pressure fuel injector indicate that diesel exhaust emissions can be reduced significantly.

2. The increasing rate of injection characteristic of the electro-hydraulic injector can provide a peak injection pressure that occurs late in the compression cycle and is conducive to reduction in oxides of nitrogen. The other characteristic is a fast end of injection that promotes reductions in HC, CO and in the soluble organic fraction of the total particulates. Conversely, too high a rate of injection, or high pressure wave reflections that might influence the intensifier/plunger travel, can increase emissions.

3. Exhaust emissions and engine performance demonstrate greater sensitivity to the duration of injection than to peak injection pressure. Shorter durations of injection effectively advance the injection event

with the electro-hydraulic system. This results in a higher rate of cylinder pressure rise (heat release) and is conducive to increased NOX formation. Higher rates of NOX formation with shorter durations of injection, as demonstrated with the electrohydraulic system, should be further explored to establish the overall effect of reduced nozzle flow area and retarded injection timing.

REFERENCES

1. Parker, R. F.: Future Fuel Injection System Requirements of Diesel Engines for Mobile Power, SAE-760125, 1976.

2. Cross, R. K.; Lakra, P.; O'Neill, C.G.: Electronic Fuel Injection Equipment for Controlled Combustion in Diesel Engines, SAE-810258, 1981.

3. Komiyama, K; et al: Electronically Controlled High Pressure Injection System for Heavy Duty Diesel Engine-Kompics, SAE-810997, 1981.

4. Rice, W.J.; and Girchenough, A. G.: Modular Instrumentation System for Real-Time Measurements and Control on Reciprocating Engines. NASA TP 1757, Nov. 1980.

5. Campbell, J.; et al.: The Effect of Fuel Injection Rate and Timing on the Physical, Chemical, and Biological Characters of Particulate Emissions from a Direct Injection Diesel, SAE-810996, 1981.

6. Funkenbusch, E. F.; Leddy, D. G.; and Johnson, J. H.: The Characterization of the Soluble Organic Fraction of Diesel Particulate Matter. SAE-790418, 1979.

7. Dezelick, R. A.: Baseline Performance and Emissions Data for a Single Cylinder, Direct Injected, Diesel Engine, NASA Technical Paper No. DOE/NASA/50194-82/1, December 1982.

TABLE I. - DF-2 REFERENCE TEST FUEL PROPERTIES

Distillation Temperature Characteristics	
Percent Recovered	Temperature, °C
Initial boiling point	191
5 percent	210
10 percent	220
20 percent	229
30 percent	245
40 percent	255
50 percent	263
60 percent	271
70 percent	280
80 percent	288
90 percent	301
Final boiling point	316

TABLE II. - ELECTRO-HYDRAULIC INJECTOR VARIATIONS - SEQUENCE TESTED

Injector A	No. of Tests	BMEP, kPa	ERPM	Description
No. 1 Sequence	2	675	2500	Accumulator supply pump pressure of 23 MPa, feed pump pressure of 2.5 MPa, and nozzle drilling of five holes at 0.36 mm diam Supply Pressure
5 hole at 0.36 mm nozzle - 23 MPa Supply Pressure				
No. 2 Sequence	6	691	2500	Accumulator supply pressure was increased to 28 MPa.
5 hole at 0.36 mm nozzle - 28 MPa Supply Pressure	4	930	2500	
No. 3 Sequence	3	873	1500	Accumulator supply pressure was increased to 33 MPa and both solenoid valves were readjusted.
5 hole at 0.36 mm nozzle - 33 MPa Supply Pressure	2	1125	1500	
	1	1300	1500	
	2	793	2000	
	2	1022	2000	
	2	1198	2000	
	3	714	2500	
	3	954	2500	
	3	1189	2500	
Injector B				
No. 4 Sequence	2	690	2500	Replacement of the five hole nozzle with an eight hole nozzle drilled for 0.25 mm diam. - 23 percent reduction in flow area. One test at 28 MPa and one test at 33 MPa supply pressure.
8 hole at 0.25 mm nozzle - 28/33 MPa Supply Pressure				
No. 5 Sequence	2	978	2500	Readjustment of both spill valve and accumulator valve solenoids because of instability at higher load - 28 MPa supply pressure
8 hole at 0.25 mm Readjusted - 28 MPa Supply Pressure				
No. 6 Sequence	3	719	2500	Replacement and readjustment of the drain valve solenoid - 28 MPa supply pressure.
8 hole at 0.25 mm - Readjusted - 28 MPa Supply Pressure	3	955	2500	

TABLE III. - SUMMARY OF DATA FROM ELECTRO-HYDRAULIC INJECTOR VS. MECHANICAL SYSTEM

Mean (Std. Dev.)

Test Sequence	No. Tests	Supply, MPa	Inpeak, MPa	Cylpeak, MPa	BMEP, kPa	A/F	BSFC	BSNOX	BSHC	BSCO	BSPM	SOF
							gm/kW-hr					
80 μL/Injection at 2500 ERPM												
Baseline	6	—	40.1	14.8	690 (6)	50 (0.5)	261 (3)	17.6 (0.8)	2.29 (0.2)	2.90 (1)	1.94 (0.9)	1.53
No. 1[a]	2	23	46.7	12.3	675 (16)	50 (2)	263 (2)	10.7 (0.3)	0.95 (0.1)	0.94 (0.3)	1.06 (0.1)	0.34
No. 2[a]	6	28	54.8	12.8	691 (19)	51 (2)	255 (2)	11.5 (0.3)	1.08 (0.5)	1.36 (0.4)	1.44 (0.5)	0.89
No. 3[a]	3	33	50.4	15.3	714 (5)	50 (0.4)	255 (1)	18.1 (1.3)	1.10 (0.1)	1.46 (0.2)	1.08 (0.1)	0.53
No. 4[b]	2	28/33	50.9/62	14.6/15	726/747	50.2/49.5	247/241	20/22	0.37/0.41	0.65/0.72	0.82/0.94	—
No. 5[b]	0	—	—	—	—	—	—	—	—	—	—	—
No. 6[b]:												
20° CA-BTC	1	28	57.6	13.8	720	47.7	260	17.0	1.39	1.70	2.53	1.04
18° CA-BTC	1	28	56.4	13.3	715	49.3	256	14.4	1.61	1.51	2.86	1.63
16° CA-BTC	1	28	55.8	12.8	722	48.5	254	12.7	1.58	2.28	2.70	1.80
100 μL/Injection at 2500 ERPM												
Baseline	6	—	51.3	14.8	955 (8)	39 (0.6)	238 (3)	17.3 (0.5)	1.84 (0.2)	3.10 (1.3)	1.41 (0.3)	0.86
No. 1[a]	0	—	—	—	—	—	—	—	—	—	—	—
No. 2[a]	4	28	55.5	13.1	930 (28)	42 (4.3)	239 (4)	10.3 (0.4)	0.67 (0.3)	1.34 (0.4)	1.37 (0.5)	0.53
No. 3[a]	3	33	53.0	15.8	954 (2.3)	39.5 (0.3)	236 (2)	17.5 (1.0)	1.09 (0.2)	1.80 (1.0)	1.16 (0.5)	0.26
No. 4[b]	0	—	—	—	—	—	—	—	—	—	—	—
No. 5[b]	2	28	60.4	13.4	978 (0.7)	40.3 (0.2)	228 (1)	11.4 (0.3)	0.47 (0.2)	0.69 (0.1)	0.46 (0.0)	—
No. 6[b]:												
20° CA-BTC	2	28/33	62.7/69.2	14.5/14.8	973/953	39.4	233/240	15.6/16.5	1.37/1.66	2.88/4.4	1.91/1.93	1.13
18° CA-BTC	1	28	61.0	13.7	944	39.1	242	12.7	1.52	3.24	1.90	1.24
16° CA-BTC	1	28	58.8	13.1	948	40.5	233	10.8	1.23	1.93	1.94	1.30

[a]With injector A - 5 holes at 0.36 mm diam

[b]With injector B - 8 holes at 0.25 mm diam

TABLE IV. - AVERAGE DATA FOR ELECTRO-HYDRAULIC INJECTOR VS. BASELINE-[ ]

(33 MPa Supply Pressure)
5 Hole nozzle at 0.36 mm diam

NO. TESTS	μL/INJ	A/F	INPEAK, MPa	CYLPEAK, MPa	BMEP, kPa	BSFC	BSNOX	BSCO	BSHC	BSPM	SOF
						g/kw-hr					
1500 ERPM - TIMING 14°CA-BTC											
3	80	55.7	50.2	16.7	873	210	25.9	1.6	0.9	1.8	1.26
3		[59.2]	[43.7]	[15.8]	[871]	[209]	[18.3]	[2.5]	[1.9]	[1.3]	[0.82]
2	100	47.2	53.2	17.5	1125	201	24.0	1.1	0.5	0.6	0.27
3		[47.4]	[47.5]	[17]	[1125]	[202]	[19.6]	1.6	[1.4]	[0.7]	[0.44]
1	120	41.2	57.9	17.6	1229	203	21	1.5	0.4	0.6	—
3		[36.4]	[45.0]	[18.1]	[1343]	[201]	[19.3]	[1.8]	[1.2]	[0.7]	[0.26]
2000 ERPM - TIMING 15°CA-BTC											
2	80	55	52.5	15.5	793	231	20.4	1.4	1.2	1.6	1.18
6		[52.8]	[43.9]	[14.6]	[781]	[232]	[15.7]	[2.4]	[1.9]	[0.9]	[0.67]
2	100	41.5	53.3	16.1	1022	223	17.6	1.7	0.9	1.2	0.77
6		[43.8]	[51.9]	[15.9]	[1026]	[221]	[17.7]	[1.7]	[1.6]	[0.8]	[0.62]
2	120	34.8	53.3	16.6	1198	218	17.0	2.3	0.7	1.2	0.43
5		[36.3]	[55.3]	[17.3]	[1254]	[217]	[18.9]	[2.3]	[1.3]	[0.8]	[0.42]
2500 ERPM - TIMING 18°CA-BTC											
3	80	49.9	51.8	15.3	714	254	18.1	1.5	1.1	1.1	0.54
6		[49.7]	[40.1]	[15.3]	[690]	[261]	[17.5]	[2.9]	[2.1]	[1.5]	[1.19]
3	100	39.5	51.6	15.8	954	236	17.5	1.8	1.1	1.2	0.26
6		[39.0]	[53.0]	[15.7	[956]	[239]	[17.5]	[3.2]	[1.7]	[1.2]	[0.73]
3	120	32.1	51.5	16.3	1189	229	16.0	2.7	0.9	1.2	0.36
6		[33.3]	[60.2]	[16.8]	[1185]	[229]	[18.0]	[4.7]	[1.4]	[0.9]	[0.50]

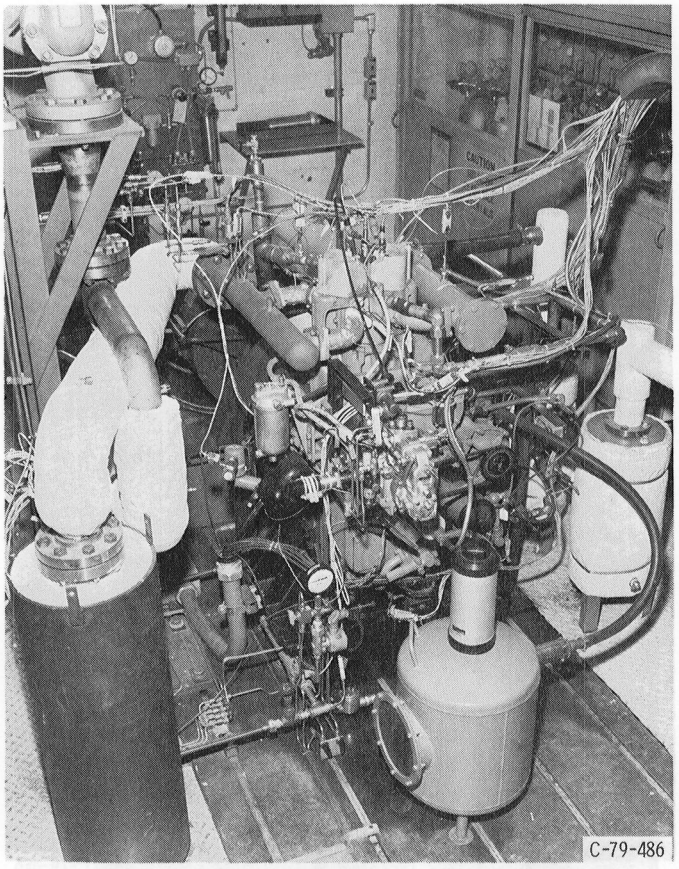

Figure 1. - Single cylinder test engine installation.

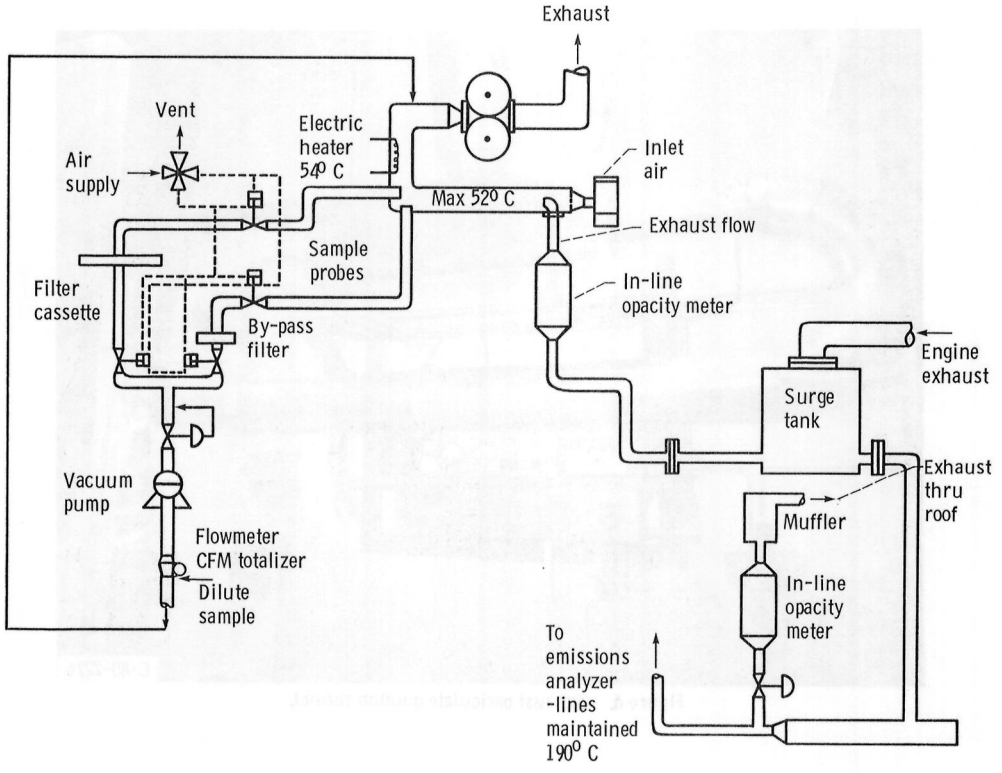

Figure 2. - Exhaust emissions sampling system.

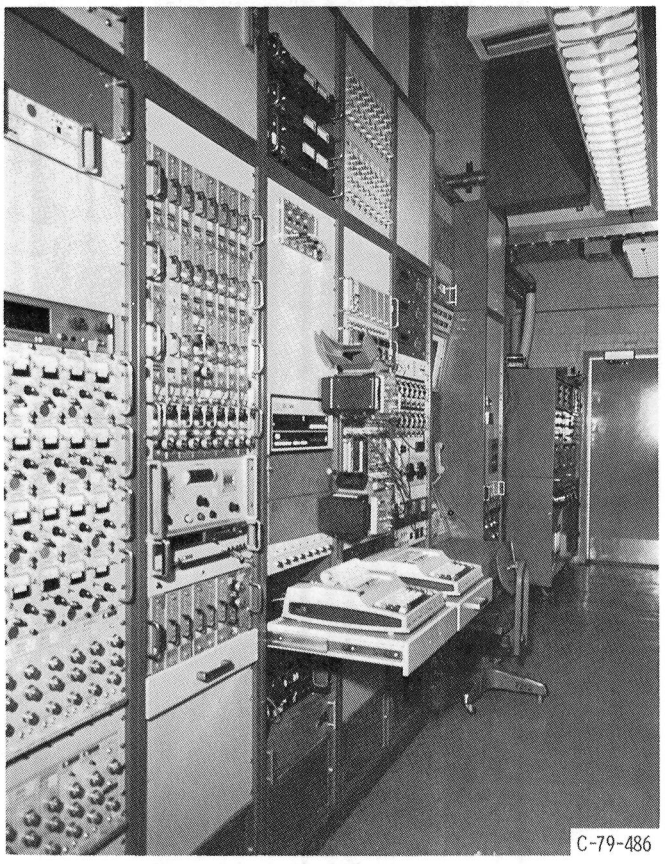

Figure 3. - NASA test operators console, instrument panel, and exhaust emissions console.

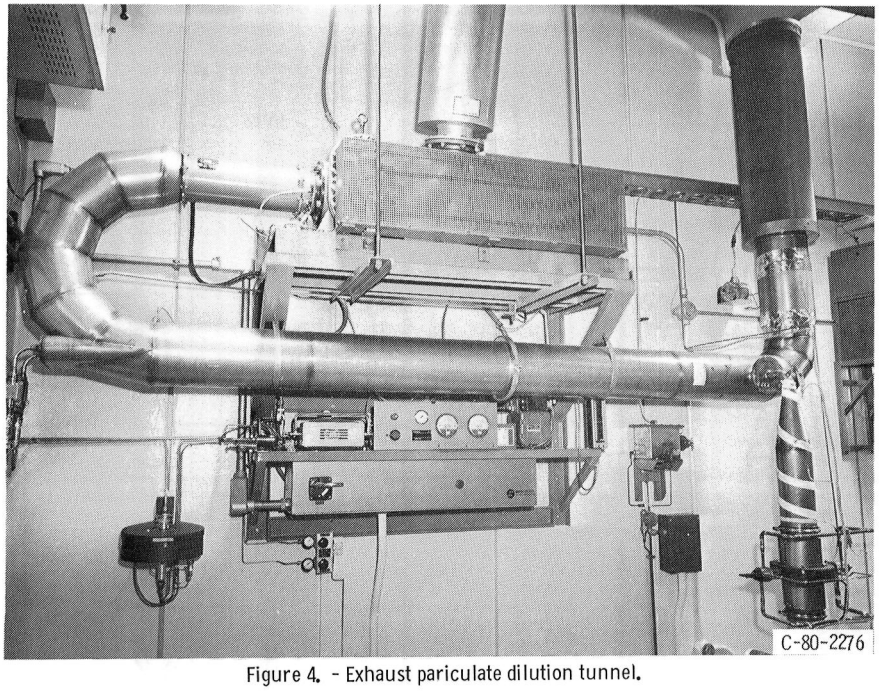

Figure 4. - Exhaust pariculate dilution tunnel.

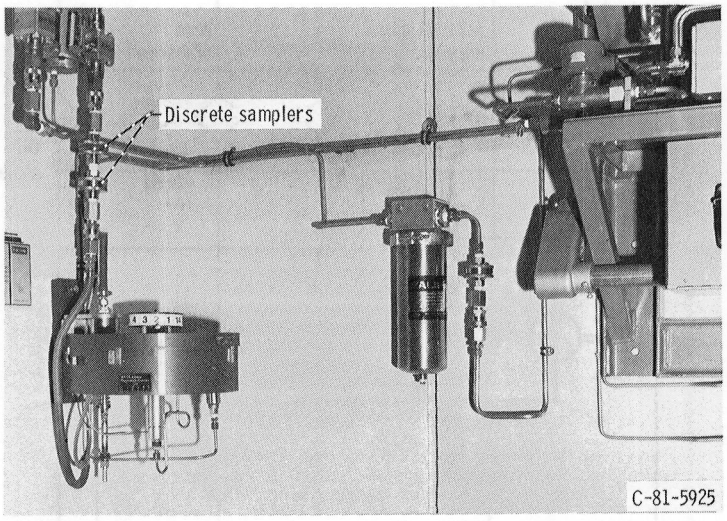

Figure 5. - Modification of remotely controlled filtering cassette to include discrete particulate samplers.

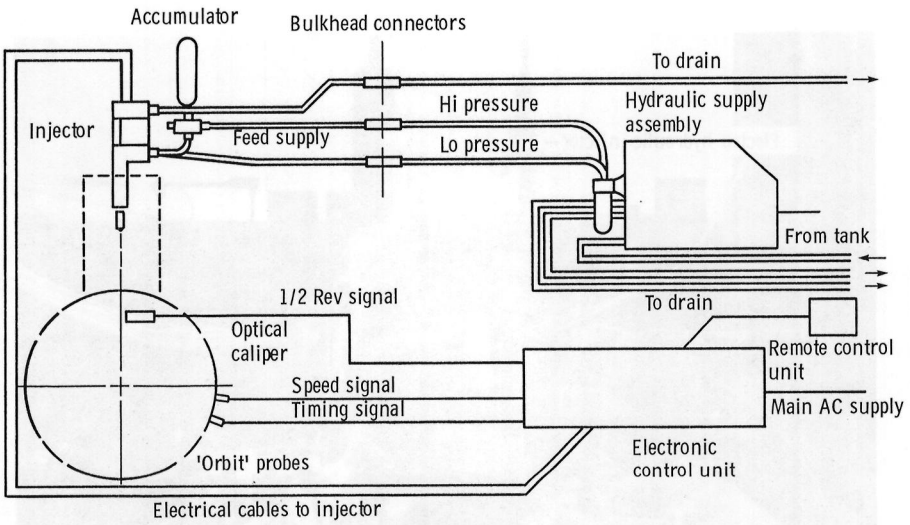

Figure 6. - Electro-hydraulic injection system.

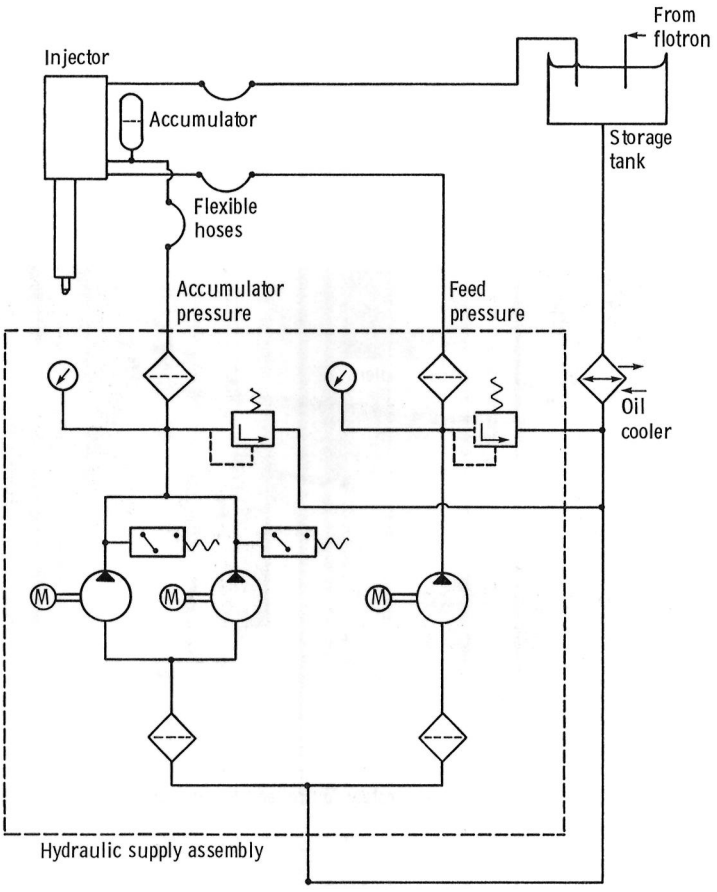

Figure 7. - Hydraulic system schematic for electro-hydraulic injection system.

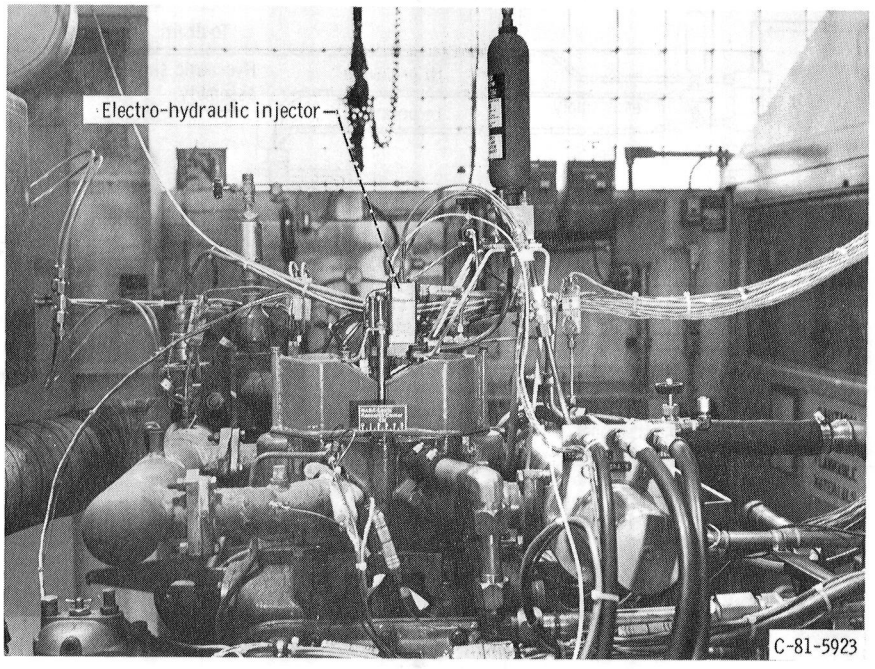

Figure 8. - Electro-hydraulic injector as installed on single cylinder test engine.

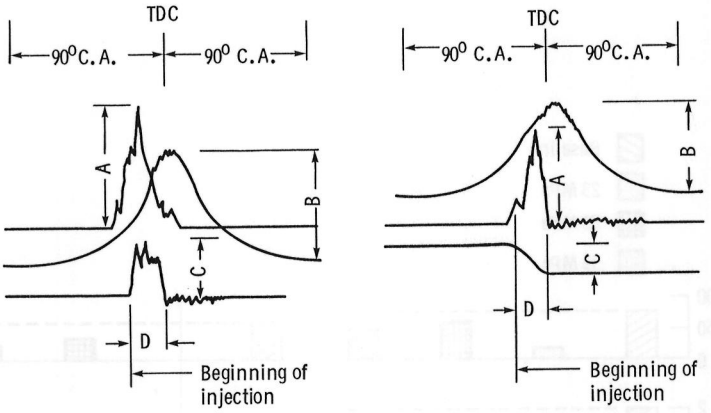

Mechanical	Injector	Electro-hydraulic
5 Holes at 0.36 mm	Nozzle drilling	5 Holes at 0.36 mm
"A" dimension	Injection peak pressure	"A" dimension
"B" dimension	Cylinder peak pressure	"B" dimension
Nozzle valve lift	"C" dimension	Plunger displacement
"D" dimension	Duration of injection	"D" dimension

Figure 9. - Cylinder gas pressure and injection pressure oscillograms as applied to both the electro-hydraulic and mechanical fuel injection systems.

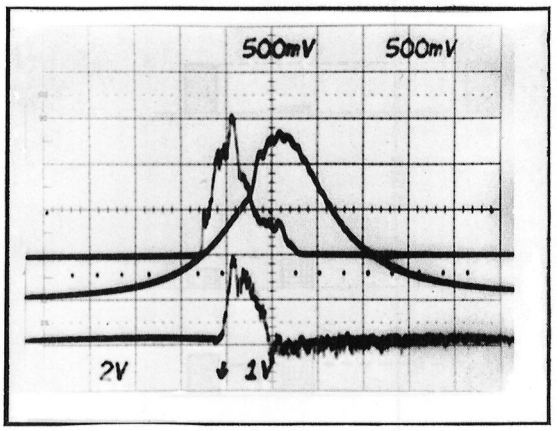

TEST #1324

Injector Configuration: Mechanical
Nozzle: 5 hole @ 0.36 mm dia.
μL/injection: 80
BMEP = 690 KPa @ 2500 RPM
Beginning of Injection = 18° BTC
INPEAK: 40 MPa @ 15° BTC
CYLPEAK: 14.8 MPa

SCALE:

Pcyl = 4.14 MPa/div
Pinj = 13.8 MPa/div
CA° = 20°/div

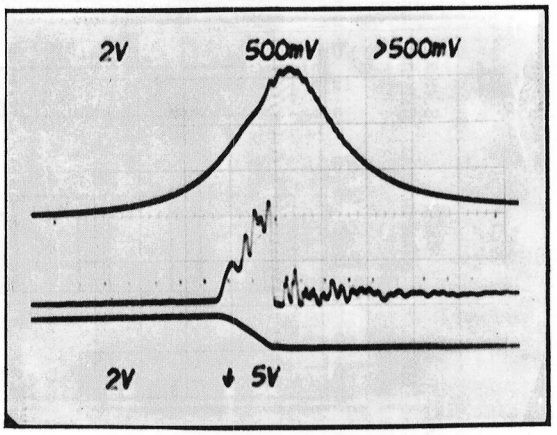

TEST #1499

Injector Configuration: Electro-Hydraulic
Nozzle: 5 hole @ 0.36 mm dia.
μL/injection: 80
BMEP = 6896 KPa @ 2500 RPM
Beginning of Injection: 18° BTC
INPEAK: 47.5 MPa @ 6° BTC
CYLPEAK: 12.6 MPa

SCALE:

Pcyl = 4.14 MPa/div
Pinj = 20.7 MPa/div
CA° = 20°/div

Figure 10. - Comparison of Electro-Hydraulic Injector to the Mechanical Baseline Injector Pressure Oscillogram for 80μL/ Injection at 2500 ERPM Using an Accumulator Supply Pressure of 23 MPa.

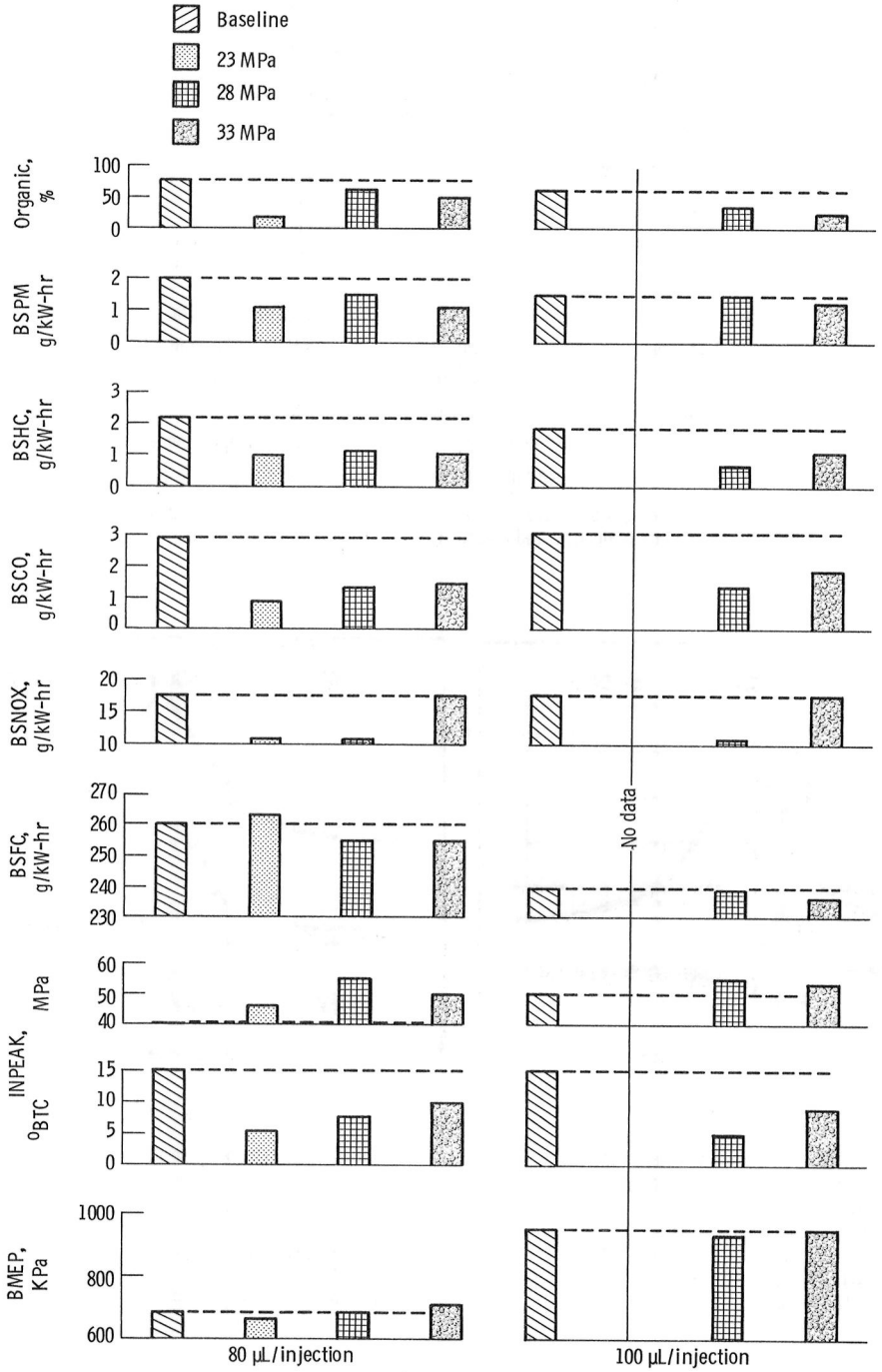

Figure 11. - Summary of test results with electro-hydraulic injector for three accumulator supply pressures: 23 MPa, 28 MPa, and 33 MPa - 80 and 100 µL/injection at 2500 erpm - versus mechanical baseline results.

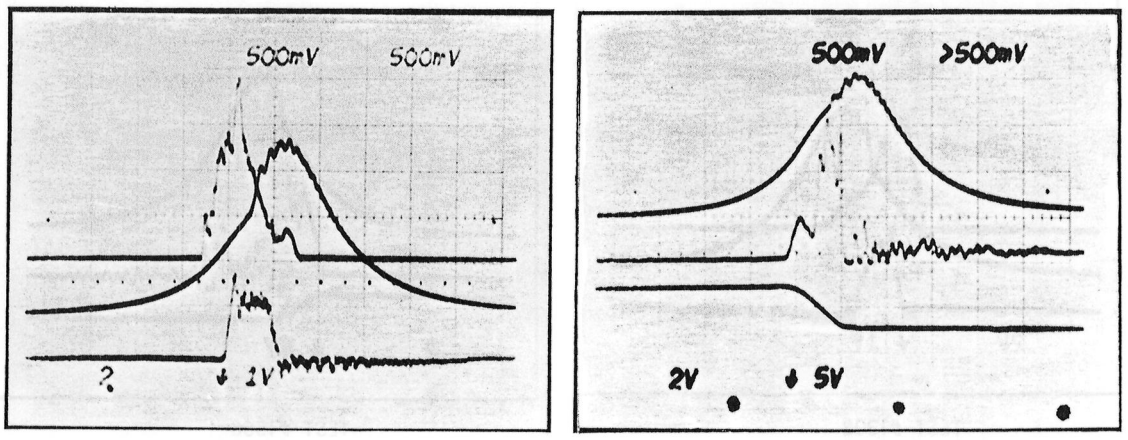

TEST #1276

Injector Configuration: Mechanical
Nozzle: 5 hole @ 0.36 mm dia.
μL/injection: 100
BMEP = 951 KPa @ 2500 RPM
Beginning of Injection = 18° BTC
INPEAK: 50.4 MPa @ 15° BTC
CYLPEAK: 15 MPa

TEST #1526

Injector Configuration: Electro-Hydraulic
Nozzle: 5 hole @ 0.36 mm dia.
μL/injection: 100
BMEP = 947 KPa @ 2500 RPM
Beginning of Injection: 18° BTC
INPEAK: 56.9 MPa @ 5° BTC
CYLPEAK: 12.98 MPa

SCALE:

Pcyl = 4.14 MPa/div
Pinj = 13.8 MPa/div
CA° = 20°/div

Pcyl = 4.14 MPa/div
Pinj = 20.7 MPa/div
CA° = 20°/div

Figure 12. - Electro-Hydraulic Injector versus Mechanical Baseline Injector Pressure Oscillogram for 100μL/Injection at 2500 ERPM Using an Accumulator Supply Pressure of 28 MPa.

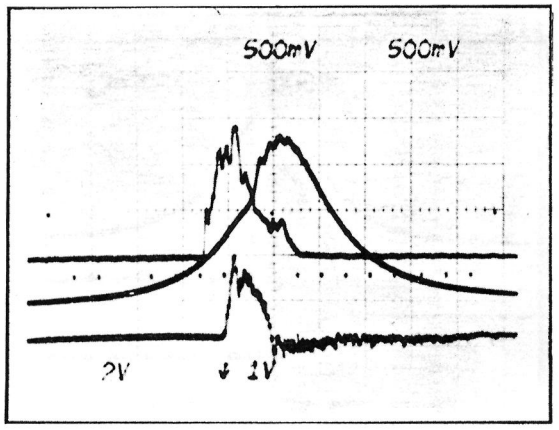

TEST #1308

Injector Configuration: Mechanical
Nozzle: 5 hole @ 0.36 dia.
µL/injection: 80
BMEP = 698 KPa @ 2500 RPM
Beginning of Injection = 18° BTC
INPEAK: 39.9 MPa @ 15° BTC
CYLPEAK: 14.8 MPa

Pcyl = 4.14 MPa/div
Pinj = 13.8 MPa/div
CA° = 20°/div

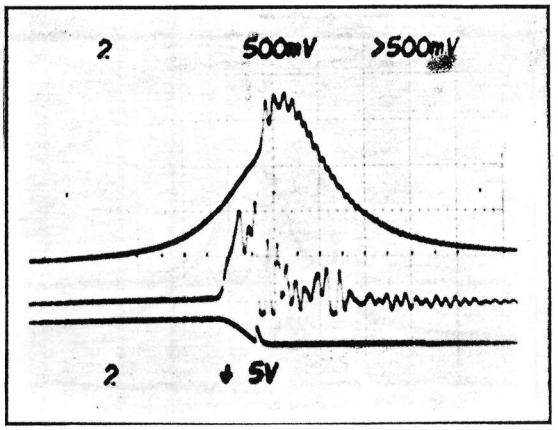

TEST #1566

Injector Configuration: Electro-Hydraulic
Nozzle: 5 hole @ 0.36mm dia.
µL/injection: 80
BMEP = 720 KPa @ 2500 RPM
Beginning of Injection: 18° BTC
INPEAK: 50 MPa @ 9° BTC
CYLPEAK: 15.2 MPa

SCALE

Pcyl = 4.14 MPa/div
Pinj = 20.7 MPa/div
CA° = 20°/div

Figure 13. - Electro-Hydraulic Injector versus Mechanical Baseline Injector Pressure Oscillogram for 80μL/Injection at 2500 ERPM Using an Accumulator Supply Pump Pressure of 33 MPa.

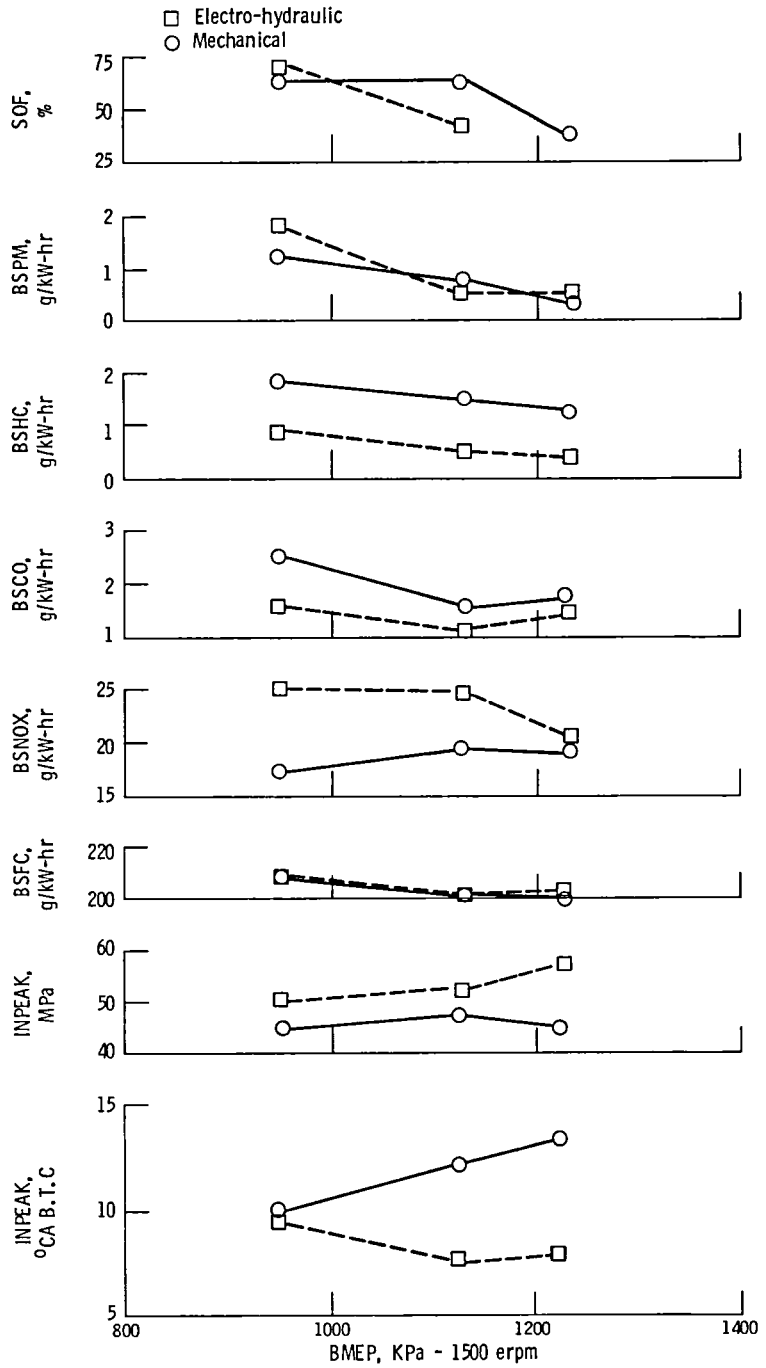

Figure 14. - Test results with electro-hydraulic injector at maximum accumulator supply pump pressure - 33 MPa - compared against baseline results at 1500 erpm.

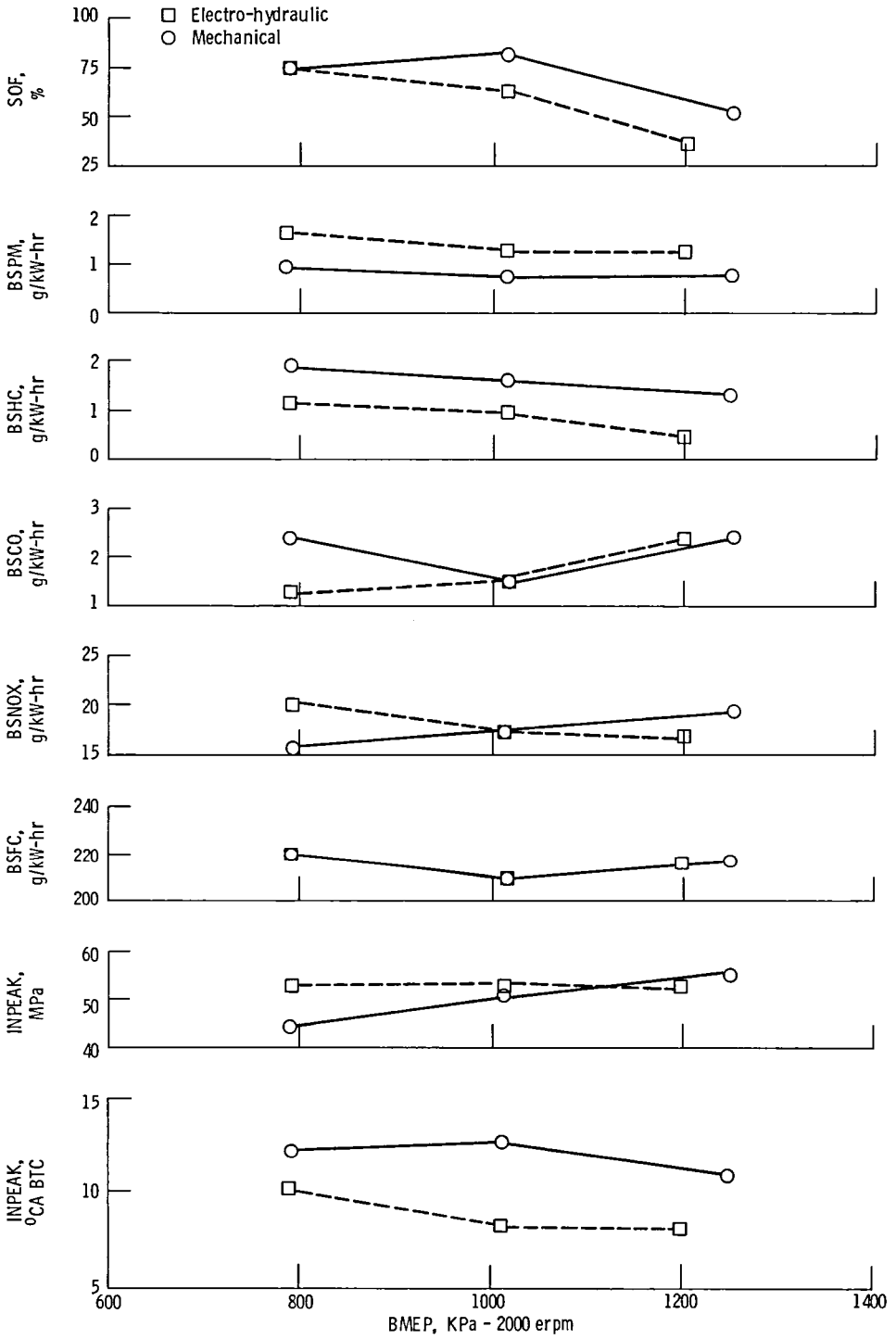

Figure 15. - Test results with electro-hydraulic injector at maximum accumulator supply pump pressure - 33 MPa - compared against baseline results at 2000 erpm.

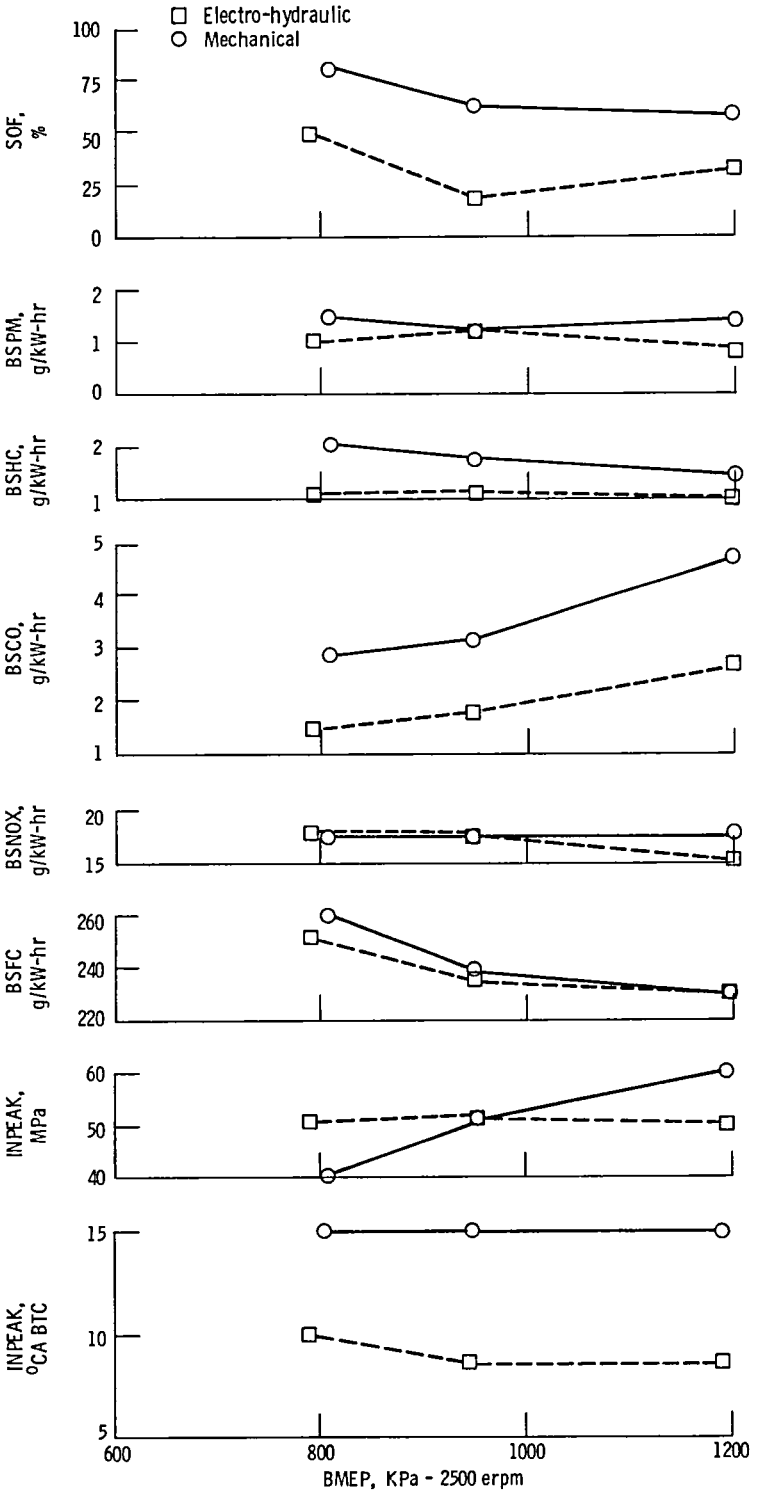

Figure 16. - Test results with electro-hydraulic injector at maximum accumulator supply pump pressure - 33 MPa - compared against baseline results at 2500 erpm.

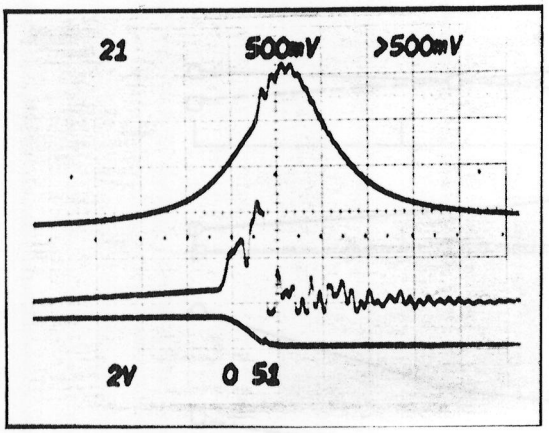

TEST #1596-28 MPa

Injector Configuration: Electro-Hydraulic
Nozzle: 8 hole @ 0.25 mm dia.
mm^3/injection: 80
BMEP = 726 KPa @ 2500 RPM
Beginning of Injection: 18° BTC
INPEAK: 51.0 MPa @ 8° BTC
CYLPEAK: 14.6 MPa
Timing pot = 3.16
Fuel pot = 8.35

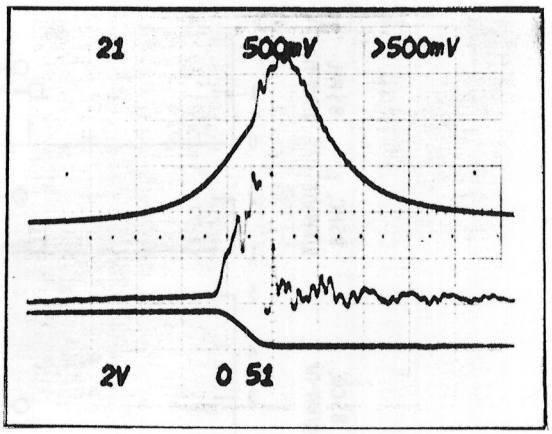

TEST #1597-33 MPa

Injector Configuration: Electro-Hydraulic
Nozzle: 8 hole @ 0.25 mm dia.
mm^3/injection: 80
BMEP = 747 KPa @ 2500 RPM
Beginning of Injection: 18° BTC
INPEAK: 62.0 MPa @ 8° BTC
CYLPEAK: 15.0 MPa
Timing pot = 3.16
Fuel pot = 8.34

SCALE:

Pcyl = 4.14 MPa/div
Pinj = 20.7 MPa/div
CA° = 20°/div

Pcyl = 4.14 MPa/div
Pinj = 20.7 MPa/div
CA° = 20°/div

Figure 17. - Electro-Hydraulic Injector Pressure Oscillogram for 80μL/Injection at 2500 ERPM Using Accumulator Supply Pressures of 28 MPa and 33 MPa.

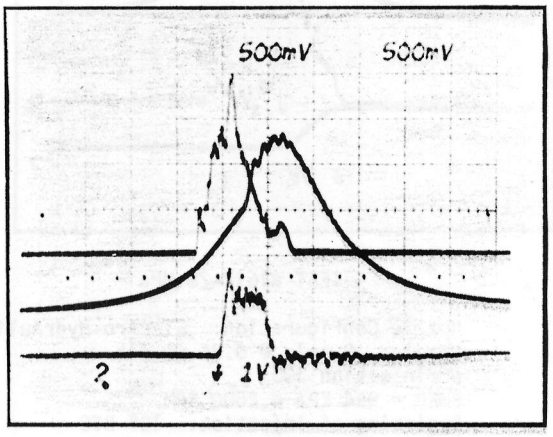

TEST #1276

Injector Configuration: Mechanical
Nozzle: 5 hole @ 0.36 mm dia.
µL/injection: 100
BMEP = 951 KPa @ 2500 RPM
Beginning of Injection = 18° BTC
INPEAK: 50.4 MPa @ 15° BTC
CYLPEAK: 15 MPa

Pcyl = 4.14 MPa/div
Pinj = 13.8 MPa/div
CA° = 20°/div

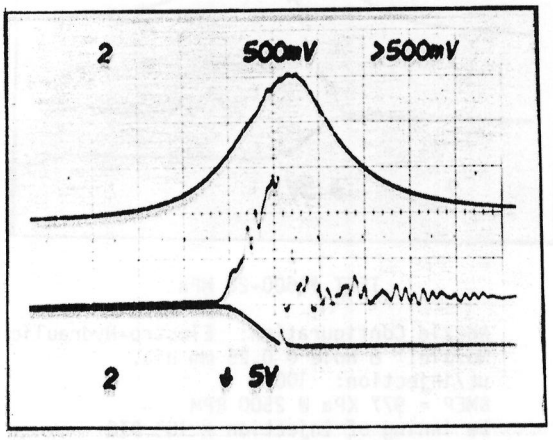

TEST # 1600-28 MPa

Injector Configuration: Electro-Hydraulic
Nozzle: 8 hole @ 0.25 mm dia.
µL/injection: 100
BMEP = 977 KPa @ 2500 RPM
Beginning of Injection: 18° BTC
INPEAK: 59.0 MPa @ 0.9° BTC
CYLPEAK: 13.4 MPa

SCALE:

Pcyl = 4.14 MPa/div
Pinj = 20.7 MPa/div
CA° = 20°/div

Figure 18. - Electro-Hydraulic Injector Configuration versus Mechanical Baseline Pressure Oscillogram for 100μL/Injection at 2500 ERPM Using an Accumulator Supply Pump Pressure of 28 MPa.

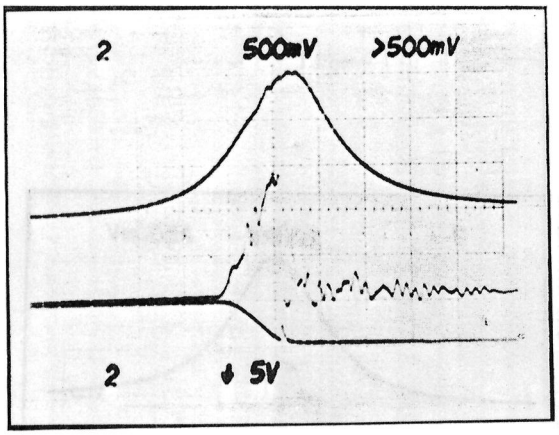

TEST #1600-28 MPa

Nozzle Configuration: Electro-Hydraulic
Nozzle: 8 hole @ 0.25 mm dia.
µL/injection: 100
BMEP = 977 KPa @ 2500 RPM
Be inning of Injection = 18° BTC
INPEAK: 59.0 MPa @ 0.9° ATC
CYLPEAK: 13.4 MPa
Timing pot = 3.16
Fuel pot = 9.04

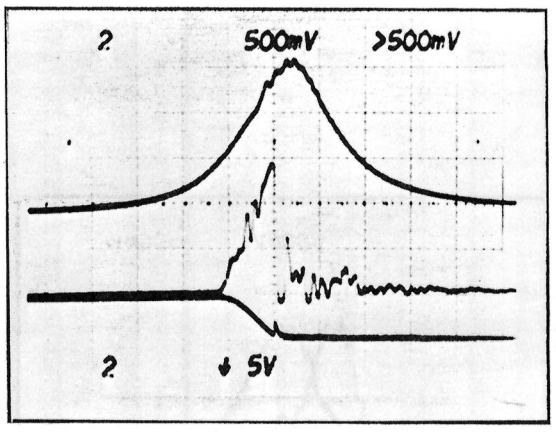

TEST #1612-28 MPa

Nozzle Configuration: Electro-Hydraulic
Nozzle: 8 hole @ 0.25 mm dia.
µL/injection 100
BMEP = 944 KPa @ 2500 RPM
Beginning of Injection: 18° BTC
INPEAK: 61.1 MPa @ 0.03° BTC
CYLPEAK: 13.7 MPa

SCALE:

Cyl Pressure = 4.14 MPa/div
Inj Pressure = 20.7 MPa/div
CA° = 20°/div

Figure 19. - Electro-Hydraulic Injector Configuration Pressure Oscillogram for 100µL/Injection at 2500 ERPM Showing the Effect on the Pressure Trace as a Result of the Adjustment of the Drain Valve Solenoid.

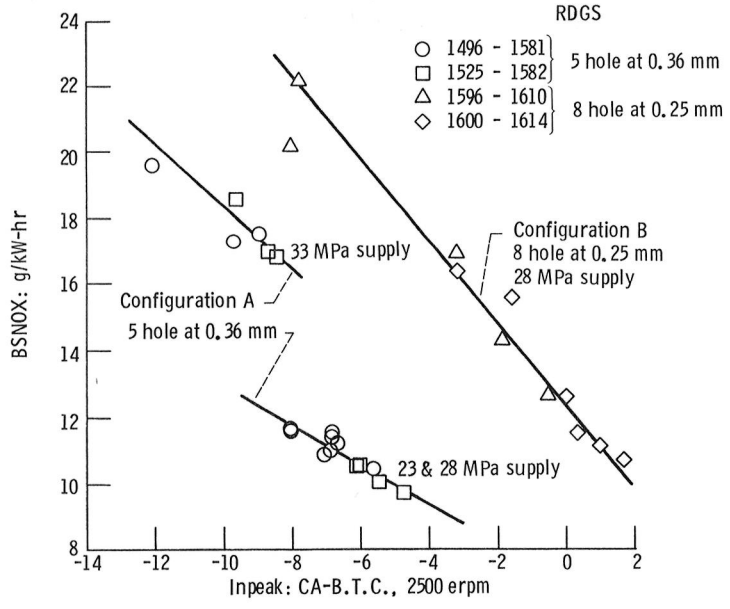

Figure 20. - Effect of peak injection pressure (INPEAK) timing on oxides of nitrogem formation at 2500 erpm.

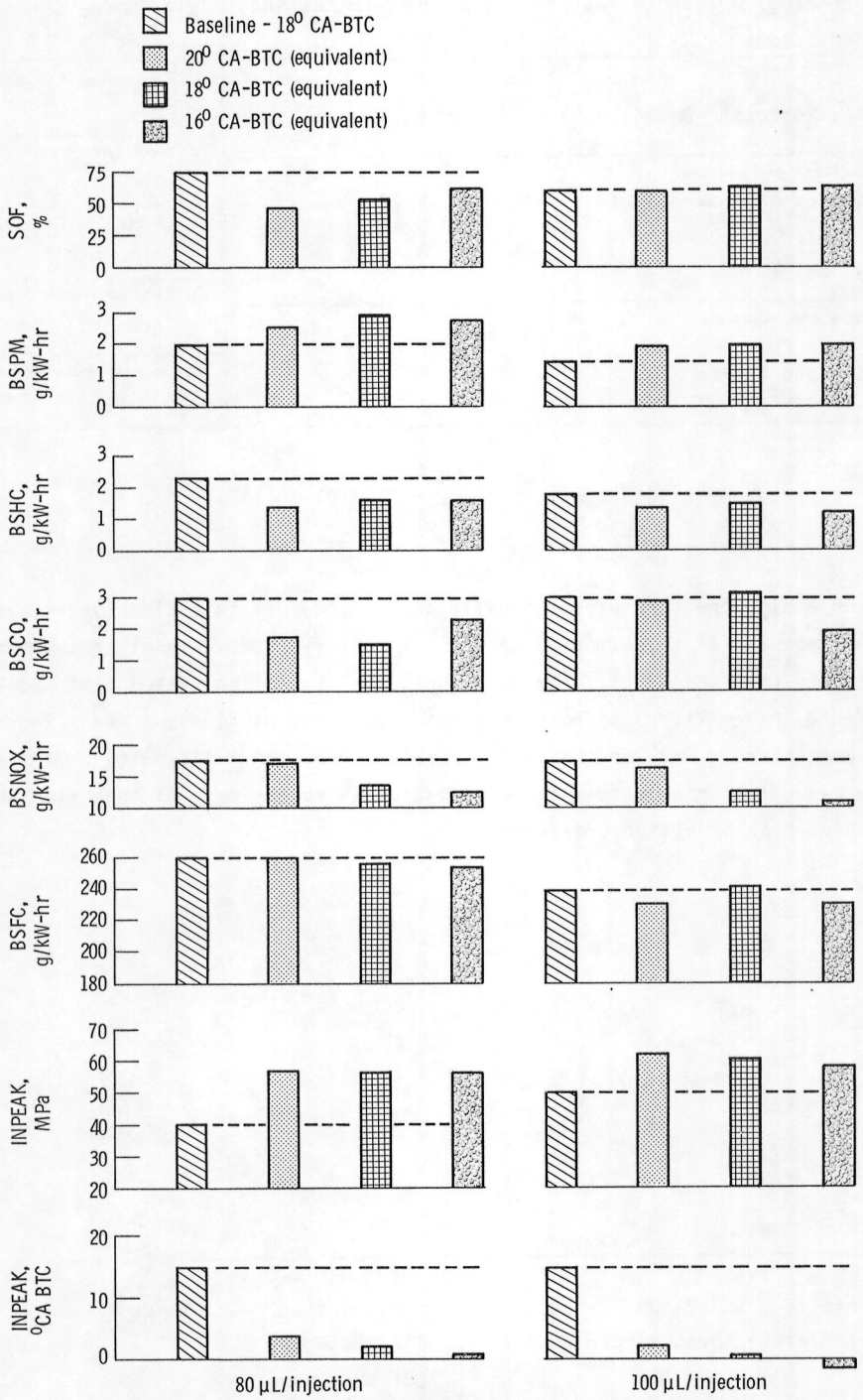

Figure 21. - Test results for electro-hydraulic injector at 3 injection timings with 8 hole nozzle at 2500 erpm compared against baseline results with 5 hole nozzle. Accumulator supply pressure = 28 MPa.

1 Report No NASA TM-83329	2. Government Accession No.	3. Recipient's Catalog No
4 Title and Subtitle Characterization of a High-Pressure Diesel Fuel Injection System as a Control Technology Option to Improve Engine Performance and Reduce Exhaust Emissions		5 Report Date March 1983 6. Performing Organization Code 778-34-22
7. Author(s) John J. McFadden, Robert A. Dezelick, and Richard R. Barrows		8. Performing Organization Report No 10. Work Unit No.
9 Performing Organization Name and Address National Aeronautics and Space Administration Lewis Research Center Cleveland, Ohio 44135		11. Contract or Grant No 13. Type of Report and Period Covered Technical Memorandum
12 Sponsoring Agency Name and Address U. S. Department of Energy Office of Vehicle and Engine R&D Washington, D. C. 20585		14. Sponsoring Agency Code Report No. DOE/NASA/50194-37

15 Supplementary Notes

Final report. Prepared under Interagency Agreement DE-AI01-80CS50194.

16 Abstract

Test results from a high-pressure electronically controlled fuel injection system are compared with a commercial mechanical injection system on a single cylinder, diesel test engine using an inlet boost pressure ratio of 2.6:1. The electronic fuel injection system achieved high pressure by means of a fluid intensifier with peak injection pressures of 47 to 69 MPa. Reduced exhaust emissions were demonstrated with an increasing rate of injection followed by a fast cutoff of injection. The reduction in emissions is more responsive to the rate of injection and injection timing than to high peak injection pressure.

17 Key Words (Suggested by Author(s)) Diesel; Electronic fuel injection; Exhaust emissions; Particulates; Turbocharged diesel; Fuel injection	18. Distribution Statement Unclassified - unlimited STAR Category 85 DOE Category UC-96		
19 Security Classif (of this report) Unclassified	20 Security Classif. (of this page) Unclassified	21. No of Pages	22 Price*

* For sale by the National Technical Information Service, Springfield, Virginia 22161